Cellular S-values for alpha-emitting radionuclides

Author: Victoria Navarro Millet, vnavarmi26@alumnes.ub.edu
Facultat de Física, Universitat de Barcelona, Diagonal 645, ES-08028 Barcelona, Spain

Advisor: José M. Fernández-Varea, jose@fqa.ub.edu

Abstract: Alpha particles are promising for radiotherapeutic purposes, given their high potency and specificity. This thesis aims to calculate cellular S-values for various source/target combinations across different cell sizes. Monoenergetic He ions and 4 radionuclides that emit alpha particles were considered. S-values were computed based on mass stopping powers from the ICRU Reports 49 and 90, with the objective of analyzing the impact of their variation under different input parameters that influence the final dosimetric outcomes. Also, the energies and yields of the alpha particles emitted in the decay of a few radionuclides of interest were taken from the ICRP Publication 107, which supersedes the older ICRP Publication 38.
Keywords: Alpha particles; targeted radiotherapy; S-values; dose point kernels; stopping power.
SDGs: This thesis is related to SDG numbers 3 and 4, notably with milestones 3.B and 3.4.

I. INTRODUCTION

Since the late 1990s and early 2000s, a new form of cancer treatment that can administer highly-localized absorbed doses, intending to induce damage or death in tumor cells, while minimizing the exposure of healthy organs and tissues, has been contemplated. This approach is known as Targeted Radionuclide Therapy (TRT), a technique intended to deliver to the nucleus of tumor cells a radiopharmaceutical agent, which consists of a radionuclide chemically bound to a carrier molecule (antibody, peptide, small molecule, etc.) where it will undergo nuclear transitions and emit ionizing radiation [1].

Research on this radiotherapeutic modality with alpha emitters has escalated in recent years, as opposed to the widespread use of beta-emitting radionuclides for TRT. Alpha particles are of interest mainly due to their short range and high linear energy transfer (LET) [2]. The implications of these properties are high precision and individuality on a specific target volume, and the capacity of inducing irreparable damage to the DNA by causing double-strand breaks with the energy transferred [3].

In this context, the principal aim of this final degree thesis is to compute cellular S-values for a few alpha-emitting radionuclides, namely ^{211}At, ^{223}Ra, ^{225}Ac, and ^{227}Th. We computed these values employing mass stopping powers (MSPs) and mass CSDA ranges provided by the International Commission on Radiation Units (ICRU) Report 49 and Report 90, and the updated energies and yields of the alpha particles emitted in their respective decay modes from ICRP Publication 107 [12].

II. MIRD FORMALISM

The Medical Internal Radiation Dose (MIRD) [4] committee, established by the Society of Nuclear Medicine (SNM), plays a central role in developing standardized methodologies for computing absorbed doses of internally-administered radiopharmaceuticals in targeted organs. Cellular S-values are coefficients, introduced in the context of internal microdosimetry, owing to their aptness when the radionuclides are confined within the cell or cell compartment. This scenario commonly arises when a radiolabeled compound is delivered into a cell when it becomes necessary to assess the absorbed dose in isolated, disseminated tumor cells. The accumulated activity $\tilde{A}$ in the source region (S) is defined as

$$\tilde{A} = \int_{t_1}^{t_2} A(t)\,\mathrm{d}t. \tag{1}$$

which produces a mean absorbed dose $\bar{D}$ to the target (T) volume articulated through the equation [5]

$$\bar{D} = \tilde{A}\,S(\mathrm{T} \leftarrow \mathrm{S}), \tag{2}$$

We considered three source regions, namely the cell nucleus, cytoplasm, and surface, where the radioactivity is homogeneously distributed. In turn, the target volume is the cellular nucleus on account of the DNA residing there. We have therefore computed $S(\mathrm{N} \leftarrow \mathrm{N})$, $S(\mathrm{N} \leftarrow \mathrm{Cy})$, and $S(\mathrm{N} \leftarrow \mathrm{CS})$.

Taking into account the proportionality between the accumulated activity and the mean absorbed dose, we can simplify by using a proportionality constant, which we assign the name of S-value expressed as [5]

$$S(\mathrm{T} \leftarrow \mathrm{S}) = \sum_i \frac{\Delta_i\,\phi_i(\mathrm{T} \leftarrow \mathrm{S})}{m_\mathrm{T}}, \tag{3}$$

where Δ_i is the mean energy emitted per disintegration, ϕ_i is the fraction of energy emitted from the source region that is absorbed in the target volume for the i-th radiation component and m_T is the mass of the target volume. This general formalism is used resulting from the consideration of having as a source a radionuclide which implies that there can be multiple emitted particles through the diverse decay mode. The calculation of

S-values with the quoted equations is usually carried out by means of time-consuming Monte Carlos simulations. When the medium is homogeneous, the expression for the S-value can be rewritten in terms of a dose point kernel (see below), which enables a much faster evaluation.

A. Dose point kernel

To accurately estimate the absorbed fraction of the dose deposited in the target volume, the dose point kernel function (DPK) is introduced. In this framework, we start modeling the radiation source as a point source immersed in an infinite, homogeneous medium with mass density ρ. Radiation is emitted isotopically and the absorbed dose to a spherical shell at a radial distance r is described by $D(r)$, the radial dose distribution. The total absorbed dose is then obtained by integrating over all the contributions of point sources within S, leading to the following expression for the S-value [6]

$$S(\mathrm{T} \leftarrow \mathrm{S}) = \frac{\rho}{m_{\mathrm{T}}} \int_0^{\infty} 4\pi r^2 D(r)\, \psi_{\mathrm{T}\leftarrow\mathrm{S}}(r)\, \mathrm{d}r. \quad (4)$$

Here $4\pi r^2\, D(r)$ represents the dose point kernel and $\psi_{\mathrm{T}\leftarrow\mathrm{S}}(r)$ is the geometric reduction factor, i.e. the probability that an isotropically-directed vector of length r that emerges from a random point within S ends in T.

B. Cell geometry

The geometric model employed to compute the cellular S-values assumes a spherical cell with a concentric spherical cell nucleus; the respective radii are R_{C} and R_{N}. Cells are seldom perfectly spherical, so that more realistic geometries such as ellipsoids should be also contemplated, but this is beyond the scope of the present thesis.

We must introduce the geometric reduction factor, $\psi_{\mathrm{T}\leftarrow\mathrm{S}}(r)$. An illustrative example is the GRF for the nucleus-to-nucleus configuration [7]

$$\psi_{\mathrm{N}\leftarrow\mathrm{N}}(r) = \begin{cases} 1 - \frac{3}{4}\,\frac{r}{R_{\mathrm{N}}} + \frac{1}{16}\left(\frac{r}{R_{\mathrm{N}}}\right)^3 & \text{if } 0 \le r \le 2\,R_{\mathrm{N}}, \\ 0 & \text{otherwise.} \end{cases} \quad (5)$$

The expressions for $\psi_{\mathrm{N}\leftarrow\mathrm{Cy}}$ and $\psi_{\mathrm{N}\leftarrow\mathrm{CS}}$ are also analytical but lenghtier.

C. Continuous-slowing-down approximation

Whilst a charged particle travels through a medium a certain distance, it undergoes small energy losses. If we disregard the energy fluctuations, the energy can be described as decreasing gradually, an approach known as the continuous-slowing-down approximation (CSDA). The loss of kinetic energy per unit path length is the stopping power of the medium, from which one deduces the CSDA range as the average distance that the particles travel until they stop. Furthermore, the trajectories are assumed to be straight lines, which is a good approximation for heavy charged particles. Hence, we can further simplify the equation for the DPK by applying the CSDA, yielding

$$4\pi r^2\, D(r) = \frac{S\big(E(r)\big)}{\rho} = \frac{1}{\rho}\left(-\left.\frac{\mathrm{d}E}{\mathrm{d}X}\right|_{X(E)}\right). \quad (6)$$

The expression then for the S-value in the CSDA is as follows [7]

$$S(\mathrm{T} \leftarrow \mathrm{S}) = \frac{1}{m_{\mathrm{T}}} \int_0^{X(E)} -\left.\frac{dE}{dX}\right|_{X(E)-r} \psi_{\mathrm{T}\leftarrow\mathrm{S}}(r)\, \mathrm{d}r, \quad (7)$$

where $-\mathrm{d}E/\mathrm{d}X$ is the MSP computed in the remaining distance of being stopped, $X(E) - r$, where r is the distance traveled and $X(E)$ is the mass CSDA range [4].

The quad function from the SciPy library, which implements the adaptive Gauss–Kronrod quadrature method, was employed to evaluate numerically this one-dimensional integral.

III. RESULTS AND DISCUSSION

A. DPKs

Following the outlined MIRD formalism, Eq. (7), the DPKs for He ions with initial kinetic energies 3, 5, and 10 MeV were computed. A linear log-log interpolation method was implemented, based on the existing data provided in ICRU Report 90 for the MSPs and the mass CSDA ranges for certain energies. To cross-check our interpolation program, we reproduced the MSPs from the tables provided by ICRU Report 90, see Fig. 4 in Appendix A. Additionally, a plot for the mass CSDA range from ICRU Report 90 is shown in Fig. 5 in Appendix A.

As shown in Fig. 1, the DPKs drop abruptly to zero when the r coincides with the mass CSDA range. It is also worth noting that the maximum deposited energy occurs near the end of the particle's path. Additionally, He ions emitted with lower initial energies initiate with a higher value as a result of being closer to their Bragg peak. [8].

B. S-values for monoenergetic He ions

S-values for monoenergetic He ions were calculated using the DPK method under the CSDA. The calculations were performed for kinetic energies ranging from 0.1 to 10 MeV using the following GRFs: $\psi_{\mathrm{N}\leftarrow\mathrm{N}}(r)$, $\psi_{\mathrm{N}\leftarrow\mathrm{Cy}}(r)$, and $\psi_{\mathrm{N}\leftarrow\mathrm{CS}}(r)$, and for 10 combinations of cell and nucleus radii $(R_{\mathrm{C}}, R_{\mathrm{N}})$. The MSPs (and mass

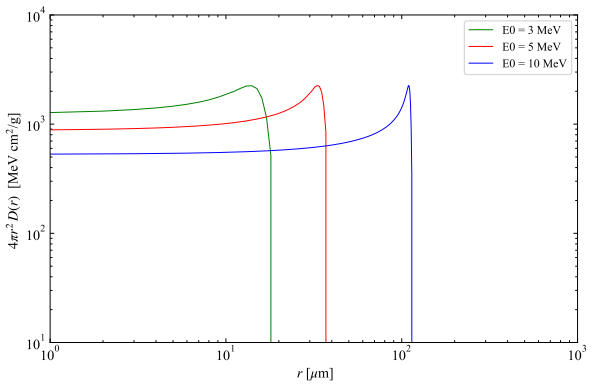

FIG. 1: Dose point kernel as a function of the radial distance for monoenergetic He ions with initial kinetic energies of 3, 5, and 10 MeV.

CSDA ranges) were taken from ICRU Repport 49, which recommends for liquid water a mean excitation energy $I = 75$ eV and a mass density $\rho = 1$ g/cm^3.

Figures 2 and 3 are representative results for a medium-sized cell ($R_C = 6$ μm) and a large cell ($R_C = 10$ μm), respectively. The present values and the reference values given by the MIRD committee [13], are evaluated using the ICRU Report 49 MSPs (and mass CSDA ranges). However, the numerical interpolation and integration method employed to compute the MIRD reference cellular S-values were not disclosed. Both sets of S-values are in excellent agreement. For geometries involving the Cy and the CS as S, the S-values have a relative error is less than 0.6% compared to MIRD references. And the relative error is below 1% for the geometry involving the cell nucleus as T. As expected, the largest S-values occur when the source region and target volume overlap. For low energies, the S-value tends to zero as there is no distance traveled in the abscence of energetic contributions.

A second set of S-values was computed following the same methodology but adopting the updated MSPs from ICRU Report 90. Aligned with our aim, we quantified the relative difference between the S-values obtained using the newer MSPs (and ensuing mass CSDA ranges) from ICRU Report 90 and those derived from the earlier ICRU Report 49. The values from these Reports differ in the mean excitation energy and density for liquid water, since ICRU Report 49 adopts $I = 75$ eV and $\rho = 1$ g/cm^3, while ICRU Report 90 adopts $I = 78$ eV and $\rho = 0.998$ g/cm^3. The deviations in the tabulated MSPs arise mainly from the different mean excitation energies used, which play a central role in the computation of the latter through the Bethe–Bloch formula, valid for $E \gtrsim 2$ MeV.

The resulting ratios, obtained for all the S-values that are being taken into account throughout this work, range from 0.98 to 0.99. That is, the S-values obtained with the currently-accepted mass stopping powers are 1%–2% lower than those.

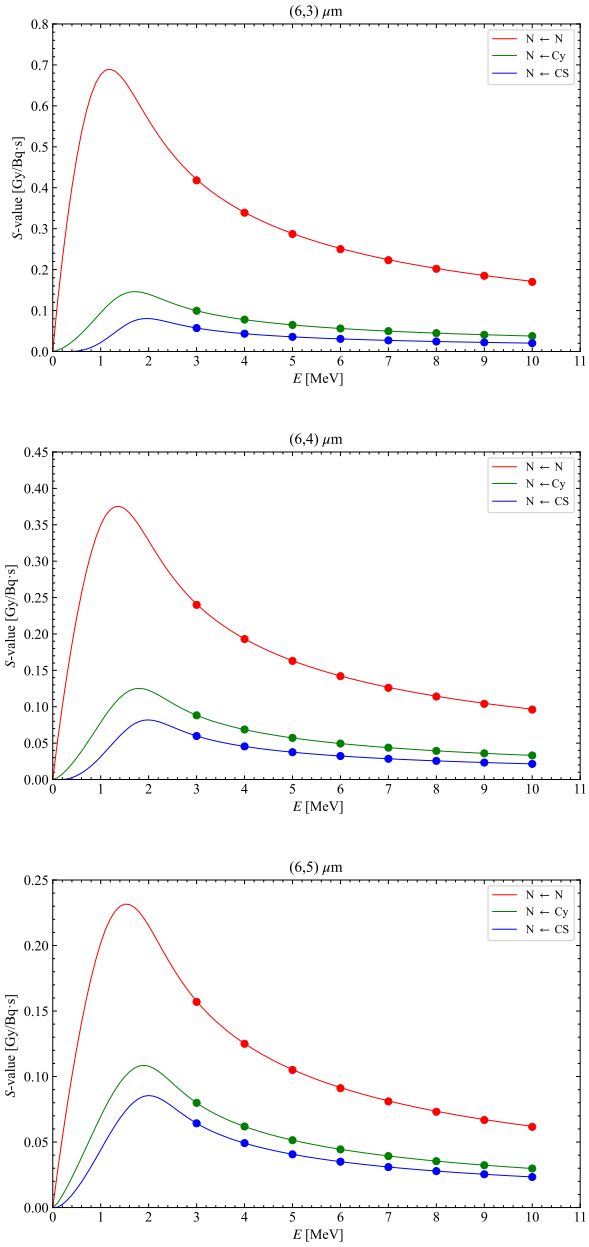

FIG. 2: S-values as a function of energy for three T←S configurations and three cell nucleus radii for a medium-sized cell. The continuous curves are the present values and the symbols are the MIRD reference values.

C. S-values for selected radionuclides

S-values were calculated for four promising radionuclides in TRT, namely ^{211}At, ^{223}Ra, ^{225}Ac, and ^{227}Th shown in Tables I and II, and in Table III in Appendix A respectively [9]. These radionuclides show therapeutic potential and are being studied, with ^{223}Ra being the first

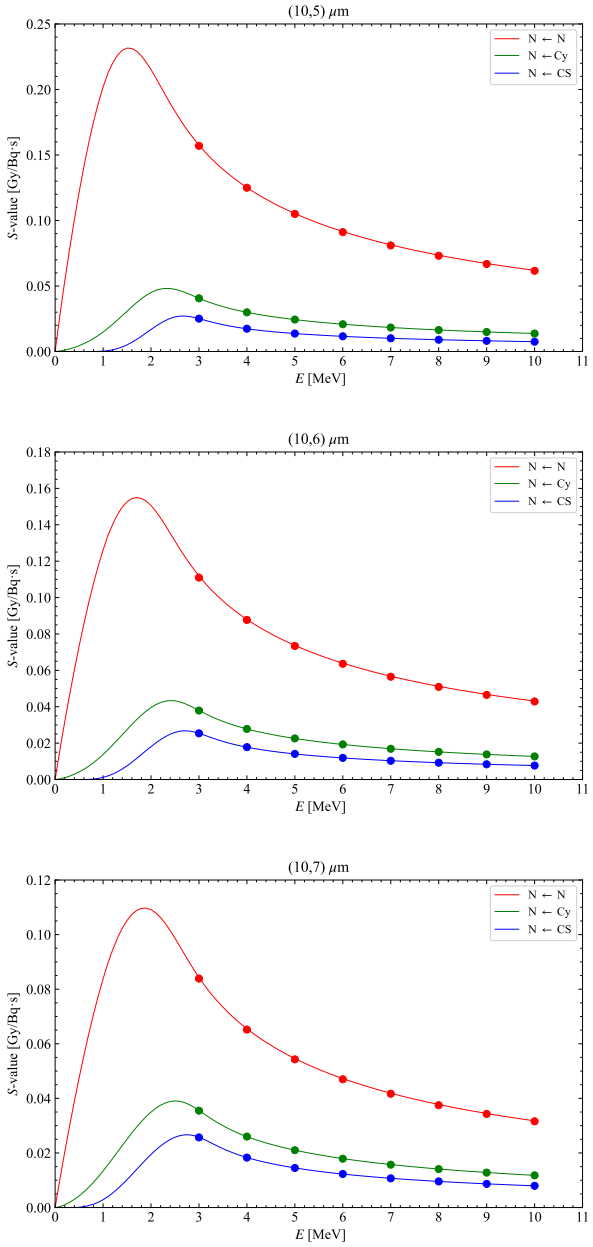

FIG. 3: S-values as a function of energy for three T←S configurations and three combinations of radii for a large cell. The continuous curves are the present values and the symbols are the MIRD reference values.

alpha-emitter approved for clinical use [10]. The ICRU Report 49 data was used to calculate these S-values, consistent with the approach taken for the MIRD reference values [13]. Additionally, the energies and intensities of radiations emitted in the decays of the aforementioned radionuclides were taken from the International Commission on Radiological Protection (ICRP) Publication 107 [12], which supersedes the decay schemes of the older ICRP Publication 38 employed in Ref. [13].

Assessing the results obtained for ^{211}At and ^{223}Ra, the best agreement with MIRD values was found in the N←Cy configuration, with discrepancies ranging from 1% to 3%. In the N←N configuration, a slight increase in the discrepancy was observed, with differences from the references between 2% and 6%, whereas the N←CS configuration shows a minor overestimation of 0.2% for larger cells. ^{225}Ac shows a consistent underestimations of 3% below the references values for all configurations.

In alignment with this project's aim, S-values were computed based on data provided by the ICRU Report 90. In the absence of MIRD reference values, the results were benchmarked against previous calculations, giving an added underestimation around 1.1% and 1.4%.

Additionally, we computed S-values for ^{227}Th based on data given by ICRU Report 49 and ICRU Report 90, shown in Table IV. Nevertheless, we can not assess discrepancies, as no reference values are provided by MIRD, despite this thorium isotope being a highly promising radionuclide in TRT and actively being under investigation and development [11].

TABLE I: S-values for ^{211}At tabulated by MIRD [13] and calculated using MSPs from ICRU Reports 49 and 90.

(R_C, R_N)		S(N ← N)	S(N ← Cy)	S(N ← CS)
(μm, μm)		(Gy/Bq·s)	(Gy/Bq·s)	(Gy/Bq·s)
(3,2)	MIRD	$2.53{\cdot}10^{-1}$	$8.42{\cdot}10^{-2}$	$5.42{\cdot}10^{-2}$
	ICRU 49	$2.39{\cdot}10^{-1}$	$8.23{\cdot}10^{-2}$	$5.34{\cdot}10^{-2}$
	ICRU 90	$2.37{\cdot}10^{-1}$	$8.14{\cdot}10^{-2}$	$5.28{\cdot}10^{-2}$
(6,3)	MIRD	$1.11{\cdot}10^{-1}$	$2.41{\cdot}10^{-2}$	$1.31{\cdot}10^{-2}$
	ICRU 49	$1.07{\cdot}10^{-1}$	$2.39{\cdot}10^{-2}$	$1.31{\cdot}10^{-2}$
	ICRU 90	$1.06{\cdot}10^{-1}$	$2.36{\cdot}10^{-2}$	$1.30{\cdot}10^{-2}$
(10,5)	MIRD	$3.99{\cdot}10^{-2}$	$8.88{\cdot}10^{-3}$	$4.92{\cdot}10^{-3}$
	ICRU 49	$3.89{\cdot}10^{-2}$	$8.87{\cdot}10^{-3}$	$4.93{\cdot}10^{-3}$
	ICRU 90	$3.85{\cdot}10^{-2}$	$8.77{\cdot}10^{-3}$	$4.87{\cdot}10^{-3}$

TABLE II: S-values for ^{223}Ra tabulated by MIRD [13] and calculated using MSPs from ICRU Reports 49 and 90.

(R_C, R_N)		S(N ← N)	S(N ← Cy)	S(N ← CS)
(μm, μm)		(Gy/Bq·s)	(Gy/Bq·s)	(Gy/Bq·s)
(3,2)	MIRD	$6.22{\cdot}10^{-1}$	$2.07{\cdot}10^{-1}$	$1.33{\cdot}10^{-1}$
	ICRU 49	$5.87{\cdot}10^{-1}$	$2.02{\cdot}10^{-1}$	$1.31{\cdot}10^{-1}$
	ICRU 90	$5.80{\cdot}10^{-1}$	$2.00{\cdot}10^{-1}$	$1.30{\cdot}10^{-1}$
(6,3)	MIRD	$2.74{\cdot}10^{-1}$	$5.94{\cdot}10^{-2}$	$3.23{\cdot}10^{-2}$
	ICRU 49	$2.63{\cdot}10^{-1}$	$5.88{\cdot}10^{-2}$	$3.23{\cdot}10^{-2}$
	ICRU 90	$2.60{\cdot}10^{-1}$	$5.81{\cdot}10^{-2}$	$3.19{\cdot}10^{-2}$
(10,5)	MIRD	$9.83{\cdot}10^{-2}$	$2.20{\cdot}10^{-2}$	$1.22{\cdot}10^{-2}$
	ICRU 49	$9.57{\cdot}10^{-2}$	$2.19{\cdot}10^{-2}$	$1.22{\cdot}10^{-2}$
	ICRU 90	$9.46{\cdot}10^{-2}$	$2.16{\cdot}10^{-2}$	$1.20{\cdot}10^{-2}$

TABLE III: S-values for ^{227}Th calculated using MSPs from ICRU Reports 49 and 90.

(R_C, R_N)		$S(N \leftarrow N)$	$S(N \leftarrow Cy)$	$S(N \leftarrow CS)$
(μm, μm)		(Gy/Bq·s)	(Gy/Bq·s)	(Gy/Bq·s)
(3,2)	ICRU 49	$5.72{\cdot}10^{-1}$	$1.97{\cdot}10^{-1}$	$1.28{\cdot}10^{-1}$
	ICRU 90	$5.65{\cdot}10^{-1}$	$1.94{\cdot}10^{-1}$	$1.26{\cdot}10^{-1}$
(6,3)	ICRU 49	$2.55{\cdot}10^{-1}$	$5.71{\cdot}10^{-2}$	$3.13{\cdot}10^{-2}$
	ICRU 90	$2.53{\cdot}10^{-1}$	$5.65{\cdot}10^{-2}$	$3.09{\cdot}10^{-2}$
(10,5)	ICRU 49	$9.30{\cdot}10^{-2}$	$2.12{\cdot}10^{-2}$	$1.18{\cdot}10^{-2}$
	ICRU 90	$9.20{\cdot}10^{-2}$	$2.09{\cdot}10^{-2}$	$1.16{\cdot}10^{-2}$

IV. CONCLUSIONS

Cellular S-values calculated in this project using the DPK method under the CSDA, based on data from ICRU Report 49, were compared with the MIRD reference tables. Our results are in good agreement with the reference values, but they exhibit a general underestimation. Larger cells with N←N configurations show the largest discrepancies.

Further calculations were performed using the same methodology, although this time employing data from ICRU Report 90. These results were compared with the ones obtained previously, as updated MIRD references are currently nonexistent. While values are in good agreement, they continue to show some slight yet significant underestimations.

Finally, S-values were computed for ^{211}At, ^{223}Ra, and ^{225}Ac, which show consistency with MIRD tabulated values based on MSPs from ICRU Report 49. Moreover, S-values were calculated for these radionuclides using the updated MSPs given by ICRU Report 90 and the updated energies and yields of the alpha particles emitted in their respective decay modes from ICRP Publication 107, considering that MIRD values are nonexistent. In addition, S-values were calculated for ^{227}Th using data from both Reports since the MIRD tables do not include this radionuclide.

Acknowledgments

I would like to express my gratitude to my supervisor, José M. Fernández-Varea, whose insightful advice and mentorship have been essential to the completion of this project. I also thank my family and friends for their unwavering and unconditional support during these years.

[1] N.K. Tafreshi, M.L. Doligalski, C.J. Tichacek, et al. Development of targeted alpha particle therapy for solid tumors. *Molecules*, 24(23):4314, 2019.

[2] S. Tronchin, J.C. Forster, K. Hickson, E. Bezak. Dosimetry in targeted alpha therapy. A systematic review: current findings and what is needed. *Physics in Medicine & Biology*, 67(9):09TR01, 2022.

[3] G. Sgouros. Alpha-particles for targeted therapy. *Advanced Drug Delivery Reviews*, 60(12):1402–1406, 2008.

[4] G. Sgouros, J.C. Roeske, M.R. McDevitt, et al. MIRD Pamphlet No. 22 (abridged): radiobiology and dosimetry of α-particle emitters for targeted radionuclide therapy. *Journal of Nuclear Medicine*, 51(2):311–328, 2010.

[5] R.W. Howell, B.W. Wessels, R. Loevinger, MIRD Committee, et al. The MIRD perspective 1999. *Journal of Nuclear Medicine*, 40(1):3S–10S, 1999.

[6] I. Scarinci, M. Valente, P. Pérez. Dose point kernel calculation and modelling with nuclear medicine dosimetry purposes. *PoS (X LASNPA)*, 84:45, 2013.

[7] S.M. Goddu, R.W. Howell, D.V. Rao. Cellular dosimetry: absorbed fractions for monoenergetic electron and alpha particle sources and S-values for radionuclides uniformly distributed in different cell compartments. *Journal of Nuclear Medicine*, 35(2):303–316, 1994.

[8] J. Kozempel, O. Mokhodoeva, M. Vlk. Progress in targeted alpha-particle therapy. What we learned about recoils release from in vivo generators. *Molecules*, 23(3):581, 2018.

[9] C.C. Oliveira-Silva, M.S. Maillard, R. Silva, L.V. Sá. Dosimetry at cellular level for the alpha-emitting radionuclides actinium-225, astatine-211 and radium-223 for bone metastasis cells from castration resistant prostate cancer. *Physics in Medicine & Biology*, 69(20):205004, 2024.

[10] C.C.O. Silva, A.X. da Silva, D. Braz, L.F.C. Lima, W.P. Segars, L.V. de Sá. S-values for radium-223 and absorbed doses estimates for $^{223}RaCl_2$ using three computational phantoms. *Applied Radiation and Isotopes*, 189:110387, 2022.

[11] V. Frantellizzi, L. Cosma, G. Brunotti, A. Pani, A. Spanu, S. Nuvoli, F. De Cristofaro, L. Civitelli, G. De Vincentis. Targeted alpha therapy with thorium-227. *Cancer Biotherapy & Radiopharmaceuticals*, 35(6):437–445, 2020.

[12] K.F. Eckerman, A. Endo. Nuclear Decay Data for Dosimetric Calculations. *Annals of the ICRP*, 38(3):e1–e25, 2008.

[13] S.M. Goddu, R.W. Howell, L.G. Bouchet, W.E. Bolch, V.D. Rao. *MIRD Cellular S Values*. Society of Nuclear Medicine, Reston, VA, 1997.

Valors S cel·lulars per a radionúclids emissors alfa

Author: Victoria Navarro Millet, vnavarmi26@alumnes.ub.edu
Facultat de Física, Universitat de Barcelona, Diagonal 645, ES-08028 Barcelona, Spain

Advisor: José M. Fernández-Varea, jose@fqa.ub.edu

Resum: Les partícules alfa són prometedores per a finalitats radioterapèutiques, donada la seva alta potència i especificitat. Aquesta tesi pretén calcular valors S cel·lulars de diverses combinacions font/objectiu per a diferents mides de cèl·lula. Es van considerar ions He monoenergètics i 4 radionúclids que emeten partícules alfa. Els valors S es van calcular basant-nos en els poders d'aturada massius dels informes ICRU 49 i 90, amb l'objectiu d'analitzar l'impacte de la seva variació sota diferents paràmetres d'entrada que influeixen en els resultats dosimètrics finals. A més, les energies i els rendiments de les partícules alfa emseses en la desintegració d'uns quants radionúclids d'interès es van extreure de la publicació ICRP 107, que substitueix la publicació ICRP 38.
Paraules clau: Partícules alfa; radioteràpia dirigida; valors cel·lulars S; nuclis de punts de dosi; poder de frenada.
ODSs: Aquest TFG està relacionat amb els Objectius de Desenvolupament Sostenible número 3 i 4, específicament amb les fites 3.B i 3.4.

Objectius de Desenvolupament Sostenible (ODSs o SDGs)

1. Fi de la es desigualtats		10. Reducció de les desigualtats	
2. Fam zero		11. Ciutats i comunitats sostenibles	
3. Salut i benestar	X	12. Consum i producció responsables	
4. Educació de qualitat	X	13. Acció climàtica	
5. Igualtat de gènere		14. Vida submarina	
6. Aigua neta i sanejament		15. Vida terrestre	
7. Energia neta i sostenible		16. Pau, justícia i institucions sòlides	
8. Treball digne i creixement econòmic		17. Aliança pels objectius	
9. Indústria, innovació, infraestructures			

El contingut d'aquest TFG, part d'un grau universitari de Física, es vincula amb l'ODS 3, i en particular amb la fita 3.B, ja que està relacionat amb la investigació i desenvolupament de noves tècniques per a malalties no transmissibles com el càncer, i també està parcialment associat amb la fita 3.4, degut a que la finalitat de la investigació és millorar la qualitat i precisió dels tractaments la qual cosa té un impacte directe en la reducció en la mortalitat. Addicionalment, també està relacionat amb l'ODS número 4, la qual intenta garantir una educació inclusiva, equitativa i de qualitat i promoure oportunitats d'aprenentatge durant tota la vida per a tothom.

Appendix A: SUPPLEMENTARY MATERIAL

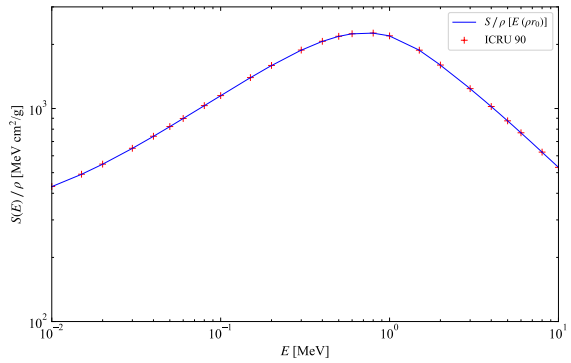

FIG. 4: MSP as a function of energy for the values provided by ICRU Report 90 and the ones computed with linear log-log interpolation.

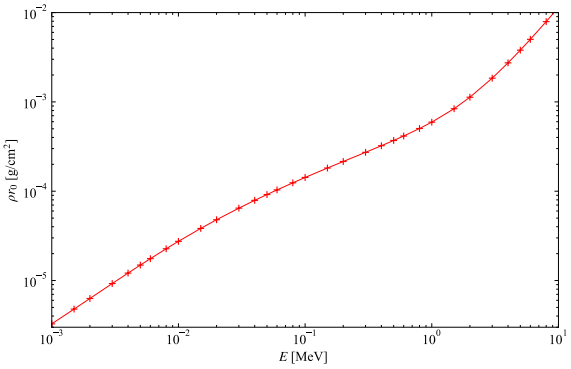

FIG. 5: Mass CSDA range as a function of energy using the tabulated values provided by ICRU Report 90.

TABLE IV: S-values for ^{225}Ac tabulated by MIRD [13] and calculated using MSPs from ICRU Reports 49 and 90.

(R_C, R_N) (μm, μm)		S(N ← N) (Gy/Bq·s)	S(N ← Cy) (Gy/Bq·s)	S(N ← CS) (Gy/Bq·s)
(3,2)	MIRD	$5.88{\cdot}10^{-1}$	$2.01{\cdot}10^{-1}$	$1.30{\cdot}10^{-1}$
	ICRU 49	$5.78{\cdot}10^{-1}$	$1.99{\cdot}10^{-1}$	$1.29{\cdot}10^{-1}$
	ICRU 90	$5.72{\cdot}10^{-1}$	$1.97{\cdot}10^{-1}$	$1.28{\cdot}10^{-1}$
(6,3)	MIRD	$2.61{\cdot}10^{-1}$	$5.81{\cdot}10^{-2}$	$3.18{\cdot}10^{-2}$
	ICRU 49	$2.59{\cdot}10^{-1}$	$5.79{\cdot}10^{-2}$	$3.17{\cdot}10^{-2}$
	ICRU 90	$2.56{\cdot}10^{-1}$	$5.72{\cdot}10^{-2}$	$3.13{\cdot}10^{-2}$
(10,5)	MIRD	$9.47{\cdot}10^{-2}$	$2.15{\cdot}10^{-2}$	$1.19{\cdot}10^{-2}$
	ICRU 49	$9.42{\cdot}10^{-2}$	$2.15{\cdot}10^{-2}$	$1.20{\cdot}10^{-2}$
	ICRU 90	$9.31{\cdot}10^{-2}$	$2.12{\cdot}10^{-2}$	$1.18{\cdot}10^{-2}$